NANO MICRO small

Supporting Information

for *Small,* DOI: 10.1002/smll.202006044

Visible-Light Induced Sustainable Water Treatment Using Plasmo-Semiconductor Nanogap Bridge Array, PNA

Emma Murphy, Yunbo Liu, Daniel Krueger, Meghna Prasad, Somin Eunice Lee, and Younggeun Park**

Supporting Information

Title: Visible-light induced Sustainable Water Treatment using Plasmo-semiconductor Nanogap bridge Array, PNA

Emma Murphy,[a‡] *Yunbo Liu,*[b‡] *Daniel Krueger,*[c] *Meghna Prasad,*[a] *Somin Eunice Lee,*[*b,d] *and Younggeun Park*[*e]

*Corresponding authors

List of supplementary information

Materials and experimental section

Materials: 2-hydroxyterephthalic acid (TAOH), terephthalic acid (TA), Methylene blue (MB), Sodium hydroxide (NaOH) were purchased from Sigma Aldrich Inc.. Polydimethylsiloxane (PDMS) were purchased from Dow chemicals Inc.. The high-purity water used was distilled, deionized and then purified with the Milli-Q system (Nippon Millipore Co., Tokyo).

Nanostructure fabrication: Firstly, we prepared a clean SiO_2 substrate by rinsing it with toluene, acetone, ethanol, and water. Between each rinsing, the SiO_2 substrate was dried out by blowing N_2 gas. With the cleaned SiO_2 substrate, we performed Au deposition (Thickness of Au layer = 5 nm and deposition rate = 0.02 nm / sec) using E-beam evaporation process (Angstrom Engineering Evovac Evaporator). Next, dewetting step followed at 450^{o}C for 30 min using a lamp-heated Rapid Thermal Process (RTP) (Jetfirst RTP 150). We confirmed that the uniform Au nanostructures (AuNS) array displayed a narrow distribution after the dewetting process by using SEM (Hitachi SU-8000). Then, we deposited TiO_2 nanolayer (Deposition rate = 0.02 nm / sec) on top of the AuNS using a E-beam evaporator (Angstrom Engineering Evovac Evaporator). A annealing process (400^{o}C) was conducted to ensure crystallinity of the TiO_2 layer[1, 2]. We next fabricated another Au nanostructure layer on top of the TiO_2/AuNS by using the same condition for the first layer of the AuNS. The morphology of the final structure was analyzed by a SEM (Hitachi SU-8000).

Particle analysis: We conducted the image processing of the SEM image using the software ImageJ. The image process consisted of scale calibration, image conversion into a binary level, identification of particles, and quantification of particle information. Firstly, we calibrated the image to correlate the image dimensions in pixel to physical dimensions. We selected the "Straight" tool from the menu bar and drew a straight line fitting the scale bar. Then, after choosing the "Set Scale" on the tab "Analyze", we clicked the "Click to Remove Scale" button, and then we filled the "Known distance" and the "Unit of Length" based on the scale

bar the SEM image. Next, we converted the SEM image into binary mode. At the tab Image, we chose “Adjust” and clicked “Threshold”. We changed the two adjustment bars to cover all particles. Next, we checked the “Dark background” box and pressed “Apply”. This process enabled the identification of particles by creating boundary lines of each particle in the SEM image. We selected “Outlines” on the “Show” selecting dialog, and marked “Display results”, “Clear results” and “Include holes”. Based on the identification, we characterized the size, interparticle distance, and density of particle by choosing “Analyze Particles” on the tab Analyze. Given that shapes of AuNS are rounded, assuming them to be of regular geometrical shapes will result in reasonable approximation.

Characterization of morphologies and optical properties: Morphologies of the PNA samples were analyzed in the acquired SEM images. The accelerating voltage was 10kV for all images. Quantitative analysis of the particle size and distribution were conducted by using ImageJ. With the fabricated structures, to obtain optical properties, a dark-field microscope was used with a dark field condenser lens (NA = 1.45, MBL12000, Nikon). The light scattered light was collected using a 20× objective lens in the microscope. Global optical properties of the samples were measured by a UV-Vis spectrometer (Agilent Technologies, Inc. Spectrometer 8453).

Construction of the integrated optofluidic device: To fabricate a micro optofluidic reactor, we used soft-lithography process. The micro optofluidic reactor consists of an inlet, an optical reaction chamber, and an outlet. To avoid collapsing of the reactor chamber, we designed 5 × 5 pillar arrays in the reaction chamber area. During the process of assembling our assay chip, we bonded the PDMS layer onto the PNA glass substrate using a medical grade double-sided tape (thickness = 20 μm) with a pattern matched the micro chamber design. After bonding the PDMS micro chamber, we performed water flow tests to confirm sealing of the assembled device.

Quantification of hydroxyl radicals: To test the generation of OH radicals under visible light illumination (Dolan-Jenner Fiber-Lite 180 with a 150W, 21 V halogen (EKE) lamp), we employed a stand scavenger reaction. When the generated OH radicals react with terephthalic acid (TA) in a basic solution, 2-hydroxyterephthalic acid (TAOH) is formed. The TAOH is emits a unique fluorescence signal at ~ 425 nm under excited at 320 nm. Therefore, the fluorescent signals associated with TAOH is linearly dependent on the concentration of the generated OH radicals[3, 4]. For the test, we filled the TA solution into the PDMS chamber (diameter = 1 cm and height = 0.5 cm). Then, we illuminated with visible light. After reaction, we collected the treated TA solution from the reactor. Next, using a microplate reader (BioTek Inc. NameSynergy Neo2), we measured intensity of the TAOH in the mixture solution. Using the same microplate reader, we constructed a calibration curve with standard TAOH solution. With the calibration curve, we quantified the concentration of the generated TAOH which represents produced OH radicals in the solution.

Visible light induced photocatalytic reaction: We estimated the photocatalytic activity of the system by employing methylene blue (MB) photodecomposition test. Having the constructed micro optofluidic reactor, first, we initiated the flow of the MB solution (10mM) into the reactor using a syringe pump (Cole Palmer, EW-74900-00). After confirming the steady state of the MB solution flowing, we illuminated visible light from the overhead lamp (Dolan-Jenner Fiber-Lite 180 with a 150W, 21 V halogen (EKE) lamp) with varying power. Then, we collected the treated MB solution from the optofluidic reactor as a function of retention time. Then, the treated MB samples were analyzed using a UV-vis absorbance spectrometer (Agilent Technologies, Inc. Spectrometer 8453) to obtain spectra and compared the peak intensity at λ = 665 nm. In addition, using the same UV-vis absorbance spectrometer, we also constructed a calibration curve with standard MB solutions. The calibration curve enabled to quantify concentration of the treated MB solution.

E. coli inactivation test: The test consisted of preparation of *E. coli* sample and inactivation test. i) Preparation of *E. coli*: Prior to the inactivation test, all samples and reactors were sterilized by autoclaving at 120 °C for 900 s. The microorganisms were cultured on a nutrient agar plate at 37 °C for 1day. The cultured bacteria were added to 10 mL of Luria-Bertani (LB) broth and incubated to reach a bacterial concentration of ~10^7 CFU/mL. The population of *E. coli* in the solution was measured with an OD meter. A portion of the solution containing the bacteria was diluted to ~5×10^6 CFU/mL with tap water. ii) Inactivation test: Before testing, similar to MB decomposition test, we initiated the flow of *E. coli* solution into the optofluidic reactor using a syringe pump. After confirming steady state flow, then, visible light was illuminated under the overhead lamp. According to the flow rate, the visible light was exposed. In the middle of exposing, we collected the treated *E. coli* solution through the outlet of the optofluidic reactor to a micro tube. To avoid addition thermal effect, the micro tube was placed in an ice box.

E. coli characterization: We performed characterization and quantification of treated *E. coli* samples. i) Characterization of *E. coli* morphology: After washing the treated *E. coli* samples with DI water, we conducted dehydration process using 50%, 60%, 70%, 80%, 90% and 100% ethanol, serially. After gentle drying, we obtained SEM images of the treated *E. coli* samples. ii) We analyzed bacteria samples using a standard spread-plate counting method.

Model local electric (*E*) field distribution: To characterize near field around PNA, we used finite element analysis (FEA, COMSOL Multiphysics software). This FEA approach is beneficial for our PNA structure for revealing the complex geometry containing many curves and asymmetric structure, owing to the ability of produce the adaptive mesh. In the pre-processing, when we constructed the computational-mesh structure, we refined the computational-mesh until the maximum electric field converged. Based on the obtained SEM images, we defined representative geometry of PNA (Au diameter = 40 nm, Au thickness =

20 nm, and interparticle distance = 40 nm) and thickness of TiO_2 layer was tuned from 1 to 30 nm. The relative permeability of gold (ε_r) was 1 and the complex permittivity of gold (ε_r) was set as a function of wavelength. The relative permeability of titanium dioxide was assumed to be ε_r = 1. The polarization vector was taken in the parallel direction to the structure of the nanostructure, whereas the direction of the k-vector was achieved to be perpendicular to the plane of the structure. A perfectly matched layer and an integration layer, modeled by concentric space, were used to reach perfect absorption at the outer boundary and minimize spurious reflections.

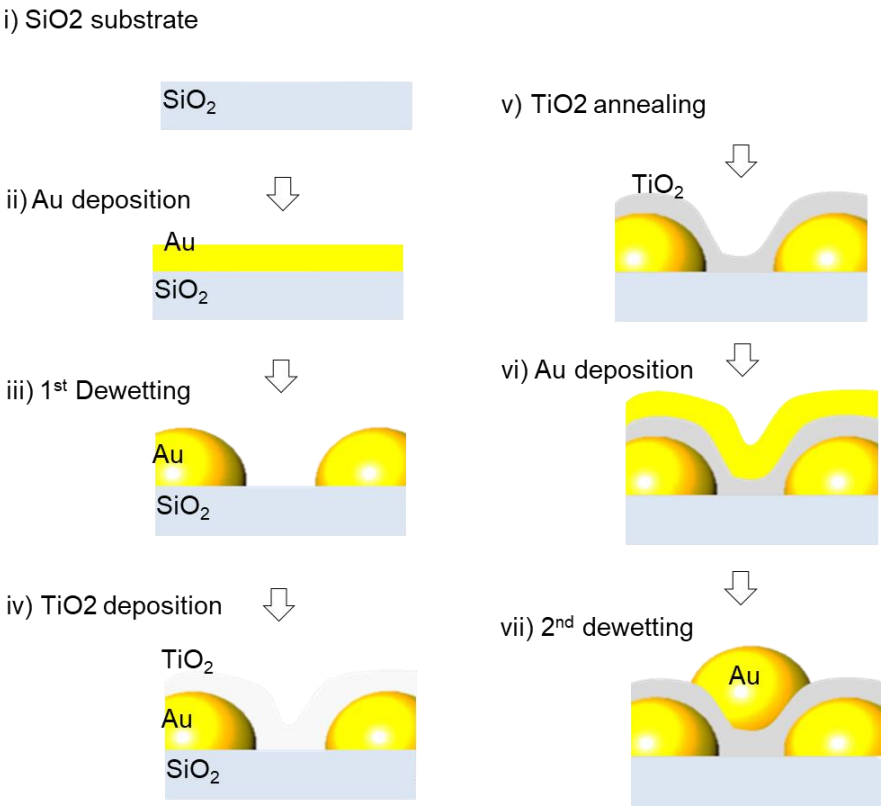

Figure S1. Large-area plasmonic nanogap of semiconductor layer fabrication process. i) Prepare clean large-area (10 cm × 2 cm) SiO_2 substrate, ii) Deposit nano Au layer on the SiO_2 substrate by E-beam evaporation (Angstrom Engineering Evovac Evaporator). iii) Conduct dewetting step followed at 450^{o}C for 30 min using lamp-heated Rapid Thermal Process (RTP) (Jetfirst RTP 150). iv) Deposit TiO_2 layer on the AuNP array. v) Anneal to ensure crystallinity of the TiO_2 layer. vi) Deposit nano Au layer on the SiO_2 substrate by E-beam evaporation (Angstrom Engineering Evovac Evaporator). vii) Conduct dewetting step followed at 450^{o}C for 30 min using lamp-heated Rapid Thermal Process (RTP) (Jetfirst RTP 150).

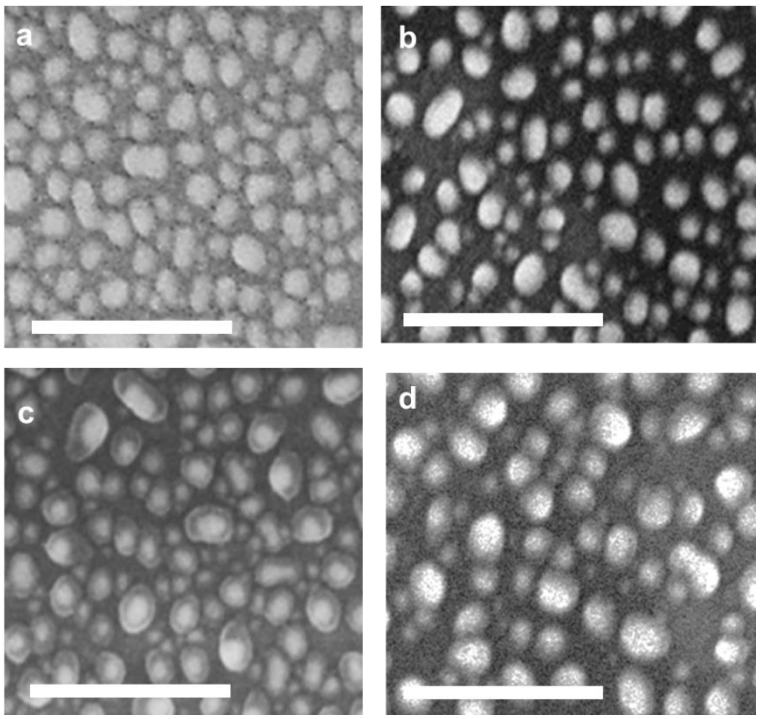

Figure S2. SEM images of PNA as a function of the $\delta_{nanogap}$ at a) 1, b) 8, c) 20, and d) 30 nm (Scale bar = 300 nm).

.

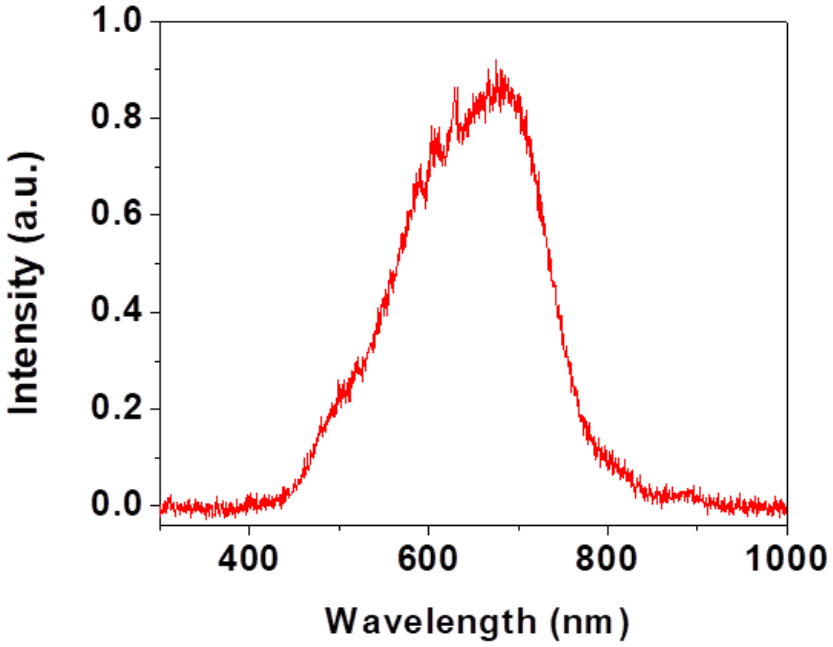

Figure S3. Visible light source spectrum. The total intensity is ~ 200 mW/cm^2 at the photo-electrode surface.

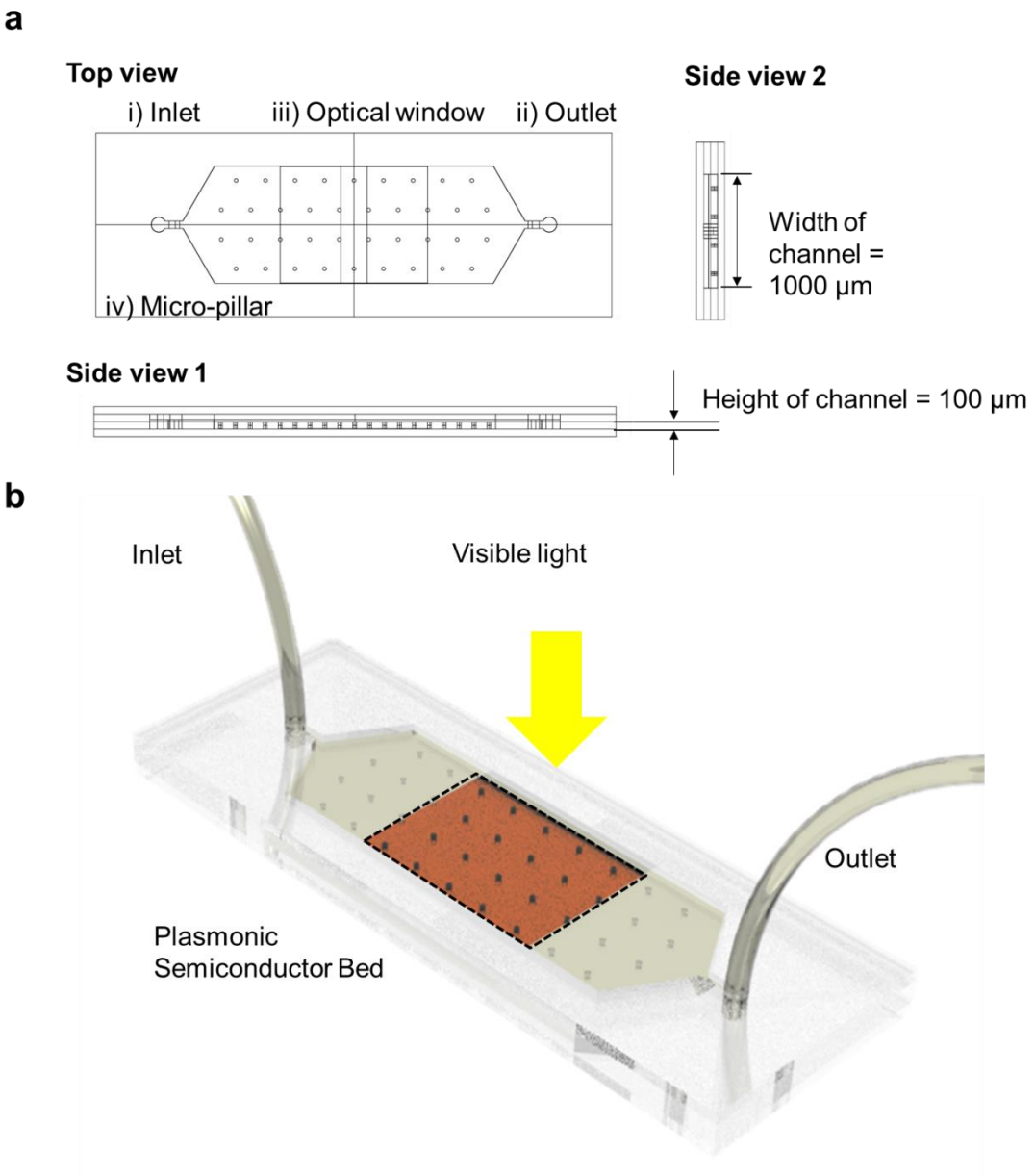

Figure S4. Optofluidic reactor design and photo image of fabricated device.

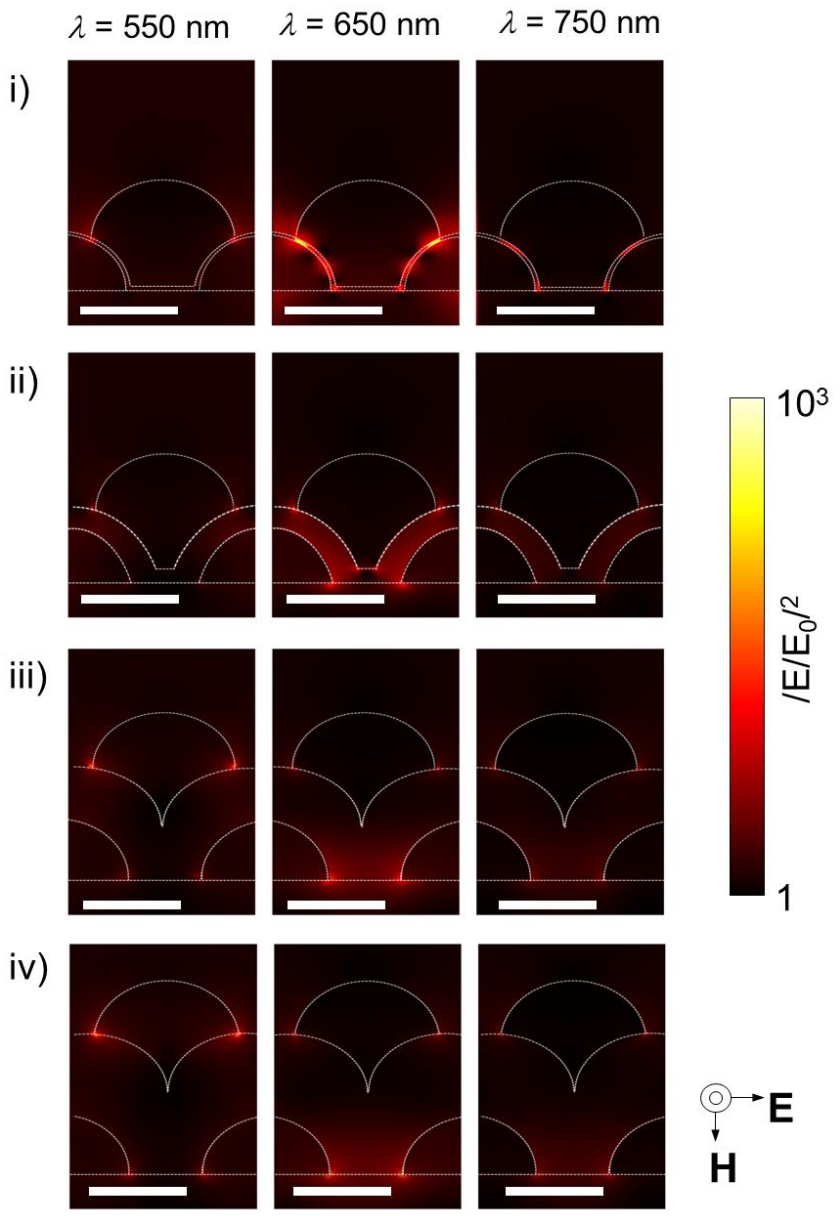

Figure S5. *E*- field distribution around PNAs with different $\delta_{nanogap}$ = i) 1, ii) 8, iii) 20, and iv) 30 nm at λ = 550, 650, and 750 nm (scale bar = 40 nm).

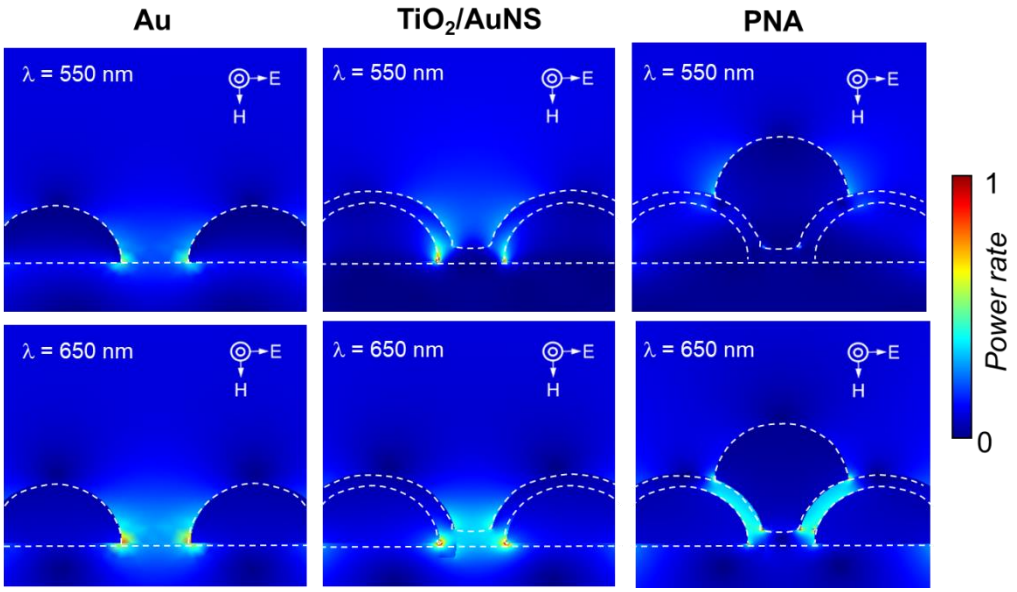

Figure S6. Power rate comparison among AuNP, TiO_2/AuNS , and PNA at λ = 550 and 650 nm at $\delta_{nanogap}$ = ~ 8 nm.

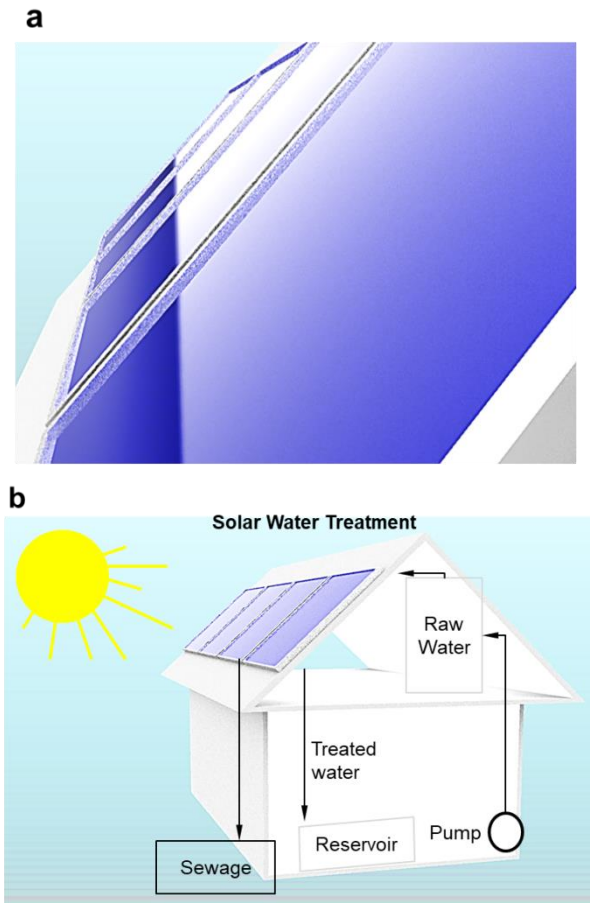

Figure S7. Decentralized optofluidic panel for sustainable water treatment process. a) Design of decentralized panel integrated with PNA **and b) schematic of water treatment process in a single house.**

Referecnes

1. Kazuya Nakata; Akira Fujishima, ***Journal of Photochemistry and Photobiology C: Photochemistry Reviews*** **2012,** ***13*** **(3), 169-189. DOI https://doi.org/10.1016/j.jphotochemrev.2012.06.001.**

2. Keiichi Tanaka; Mario F. V. Capule; Teruaki Hisanaga, ***Chemical Physics Letters*** **1991,** ***187*** **(1), 73-76. DOI https://doi.org/10.1016/0009-2614(91)90486-S.**

3. Stephen A Timko; Cristina Romera-Castillo; Rudolf Jaffé; William J Cooper, ***Environmental Science: Processes & Impacts*** **2014,** ***16*** **(4), 866-878.**

4. Behnaz Razavi; Sihem Ben Abdelmelek; Weihua Song; Kevin E O'Shea; William J Cooper, ***Water research*** **2011,** ***45*** **(2), 625-631.**